

Chemical, Petroleum and Environmental Engineering

Estimating Pitting Corrosion Depth and Density on Carbon Steel (C-4130) using Artificial Neural Networks

Rusul Kh. Abd*

Ph D. Student

Polymers And Petrochemical Engineering Dep.
Basrah University For Oil And Gas
Iraq -Basrah

rusul.alhamad@buog.edu.iq

Nawal J. Hammadi

Asst. Prof Dr.

College of Engineering – University of Basrah
Iraq –Basrah

drnawaleng@yahoo.com

ABSTRACT

The purpose of this research is to investigate the impact of corrosive environment (corrosive ferric chloride of 1, 2, 5, 6% wt. at room temperature), immersion period of (48, 72, 96, 120, 144 hours), and surface roughness on pitting corrosion characteristics and use the data to build an artificial neural network and test its ability to predict the depth and intensity of pitting corrosion in a variety of conditions. Pit density and depth were calculated using a pitting corrosion test on carbon steel (C-4130). Pitting corrosion experimental tests were used to develop artificial neural network (ANN) models for predicting pitting corrosion characteristics. It was found that artificial neural network models were shown to be quite effective; the results were validated by the experimental agreement with those acquired from laboratory tests. Specifically, the correlation coefficient, $R = 0.9944$.

Keywords: Pitting Corrosion, Carbon Steel, Pits Depth, Pit Density, ANNs.

تقدير عمق وكثافة التآكل التنقري على الصلب الكربوني (C-4130) باستخدام الشبكات العصبية الاصطناعية

م.د. نوال جاسم حمادي
استاذ مساعد متقاعد
جامعة البصرة

م.م. رسل خالد عبد
طالب دكتوراه
جامعة البصرة للنفط والغاز

الخلاصة

الغرض من هذا البحث هو دراسة تأثير كل من كلوريد الحديدية بتركيز (1 ، 2 ، 5 ، 6٪ بالوزن) عند درجة حرارة 27 ± 2 درجة مئوية ، ولفترات عمر (48 ، 72 ، 96 ، 120 ، 144 ساعة) وخشونة السطح على خصائص التآكل التنقري للفولاذ الكربوني (C-4130)، واستخدام النتائج لإنشاء خلية عصبونية واختبار امكانييتها في تخمين خصائص التآكل التنقري في مختلف الظروف . تم حساب كثافة الحفرة وعمقها بعد اجراء تجربة التآكل التنقري على الفولاذ الكربوني. حيث تم استخدام نتائج اختبارات التآكل التنقري لتطوير نماذج الشبكة العصبية الاصطناعية (ANN) للتنبؤ بخصائص التآكل التنقري حيث وجد ان نماذج الشبكة العصبية الاصطناعية فعالة جدا في التنبؤ بخصائص التآكل التنقري. تم التحقق من صحة النتائج بمقارنتها مع تلك التي تم الحصول عليها من الاختبارات المختبرية .

*Corresponding author

Peer review under the responsibility of University of Baghdad.

<https://doi.org/10.31026/j.eng.2022.05.02>

This is an open access article under the CC BY4 license (<http://creativecommons.org/licenses/by/4.0/>).

Article received: 9/10/2021

Article accepted: 9/1/2022

Article published: 1/5/ 2022



الكلمات الرئيسية: التاكل التنقري , الفولاذ الكربوني , عمق التنقر , كثافة لتنقر , الشبكة العصبية الصناعية .

1. INTRODUCTION

Corrosion deterioration drastically decreases the materials' operational life. Pitting corrosion is one of the types of corrosion that will substantially cause pollution and has the potential to explode, resulting in significant economic losses both directly and indirectly (**Ghidini and Donne, 2009**). On the other hand, pitting is a complicated process that involves many complex phenomena such as mass transfer, metal dissolution, and passivation, among others. The influencing factors of pitting corrosion are numerous, including metal components, medium temperature, pressure, pH, and the type and concentration of ions, making pitting corrosion modeling more difficult (**Choi et al., 2005, Li et al., 2012, and Qu Z et al., 2021**). It's a harmful and unexpected phenomenon. Because of the complicated effect generated by grain boundaries, inclusions, and crystallographic imperfections, a pit might form at a microscopic level at a difficult to anticipate spot on the metal surface. If optimal requirements are met, the pit grows at an extraordinarily fast rate in contrast to its size, eventually resulting in a severe metal break (**Bhandari et al., 2015, Kolawole et al., 2016, Boucherit and Tebib, 2005, and Jiménez-Come et al., 2015**). Many publications on pitting corrosion attempt to explain the reasons, mechanisms, and solutions.

Although Artificial Neural Networks (ANNs) are frequently utilized for modeling and prediction problems of corrosion in general and pitting depth in particular, just a few studies use ANNs for pitting corrosion in carbon steel (**M.E.A. BenSeghier et al., 2021**). The main objective of this study is to look into the pitting corrosion characteristics of carbon steel (C-4130) based on experimental and theoretical collected data. Metal roughness measurements, pitting corrosion tests, and pit evaluation are part of the experimental procedure. The pitting corrosion test is used to generate pits on the surface of the specimens; the surface roughness is a variable in the pitting corrosion test.

The theoretical study includes using computer software to create artificial neural network (ANN) models (Matlab 2007). The experimental results were utilized to train and test artificial neural networks that predicted the behaviour of carbon steel pitting corrosion behavior. (**M. Mohammad, J. Hammadi, and M. Lafta, 2012, and Boucherit et al., 2019**).

2. EXPERIMENTAL WORK

The material used in the present study was a carbon steel tube which was taken from the boiler furnace wall tube (Najibia Power Station-Basrah). The chemical composition (wt.%) of the tube, which is performed by the "Iben-Majed company- Basrah" is

Elements	C	Fe	Mn	Cr	Si	P	S	Mo	Cu	V
Result	0.21	98.3	0.728	0.097	0.259	0.005	0.024	0.015	0.108	0.004

In order to train ANN, it is required to have a database containing a set of input data and the corresponding target for that more than one hundred specimens of carbon steel(C-4130) they were machined as flat specimens with a square cross-section of 1.4 mm in length and were used in pitting corrosion tests. A surface finish was applied to the specimens to varying degrees. Each specimen was ground with varying grits of emery paper to achieve various degrees of



surface roughness, then polished with a polishing machine (Struers Knuth-Rotor-3), using successively changing grades of abrasive paper. The preliminary polishing steps alternated longitudinal and circumferential polishing to ensure that longitudinal scratches caused by coarser grades of abrasive materials were eliminated. The specimens were examined as received in their final condition. Visual inspection of the surface of the test sections was conducted at a magnification power of 20X using an optical microscope (Olympus, Japan) to check if there were any transverse cracks or machining marks. Then the specimens' dimensions were measured. The surface roughness measurements for the specimens were performed using a surface roughness tester portable-type (Qualitest TR-110, US) in terms of surface roughness factor (Ra) in (m).

2.1. PITTING CORROSION TEST:

The corrosive environment was applied to freshly manufactured specimens having a surface area of 1.96 cm². The pitting corrosion method involves immersing specimens in various concentrations of corrosive ferric chloride (1, 2, 5, 6, % wt.) at room temperature for 48, 72, 96, 120, and 144 hours in each concentration. The application of ferric chloride to specimens promotes pitting corrosion in the presence of aggressive chloride ions. This test was performed according to the method given by the **ASTM G48-2005** standard. This method covers the procedure for determining the pitting corrosion resistance of carbon, stainless, and alloy steel when exposed to oxidizing chloride environments. The pitting corrosion test involves the following principal steps:

1. Using different quantities of reagent grade ferric chloride, FeCl₃.6H₂O, in a certain amount of distilled water to give different ferric chloride concentrations.
2. Filtration of ferric chloride solution was done through filter paper to remove insoluble particles.
3. Measurements of the dimensions of the specimens and the total exposed surface areas were calculated.
4. Cleaning specimen surfaces with magnesium oxide paste and rinsing well with water, followed by dipping in acetone (or methyl alcohol), followed by air-drying.
5. The specimens were immersed in the test solution. The containers are covered with a watch glass.
6. Test Interval: Different test periods were adapted to investigate the effect of immersion time on pitting corrosion.
7. Cleaning after immersion: To remove corrosion products, the specimen was rinsed with water and scrubbed with a plastic bristle brush under running water, followed by dipping in acetone (or methanol) and drying.



2.2. PITTING CORROSION EXAMINATION AND EVALUATION

Examination and evaluation of pitting corrosion was conducted according to ASTM G46-2005 standard specifications (**ASTM Standards G46, 2005**). A visual examination of the corroded metal surface was carried out under ordinary light, with the use of a low-power magnifying glass (20X), to determine the extent of corrosion and the apparent location of pits. The examination procedure includes the following steps:

1. Pitting density: The pitting density was determined by using a plastic grid. The plastic grid, containing 3 mm squares, was placed on the metal surface. The number of pits in each square was counted and recorded, and then the grid was moved across systematically until the entire surface had been covered.
2. Pitting depth: The pit depth is determined by measuring the thickness difference before and after pitting corrosion. The thickness of specimens was initially measured, then the specimens were polished using a coarse grade of abrasive until all pit traces were removed, then re-measuring the thickness of the specimens and the loss thickness was considered the maximum pit depth.

3. ARTIFICIAL NEURAL NETWORKS

The most important goal during the modeling process of the ANN is to obtain the best connection between input and output variables. The ANN is a machine learning technology that is commonly used to approximate nonlinear mathematical functions (**Hornik et al., 1989, and Kh. Hussein, 2015**). The pitting characteristics, which are the output data, are represented by pitting density (pits/cm²) and pit depth (mm) in artificial neural network modeling. The inputs are the concentration of ferric chloride (corrosive solution) (%), soaking period (h), and roughness factor (m). The model's training and testing data were derived from the current study's experimental work. **Fig. 1** depicts the construction of a neural network model. It consists of three nodes in the input layer. Two hidden layers are selected, which give the minimum mean square error (MSE) and maximum correlation coefficient. The first hidden layer has sixteen nodes, and the second hidden layer has nine nodes. The output layer has two nodes, which are represented by pitting density and pit depth.

The results of artificial neural network predictions of pitting corrosion features are demonstrated to agree well with experimental data. The proper function used for both the first and the second hidden layers is (tansig), and the output layer is (purelin). The best results were obtained through trial and error until the best results were obtained by reaching the mean square error and maximum correlation coefficient lowest values. Specifically, the correlation coefficient, $R = 0.9944$, is shown in Fig.2.

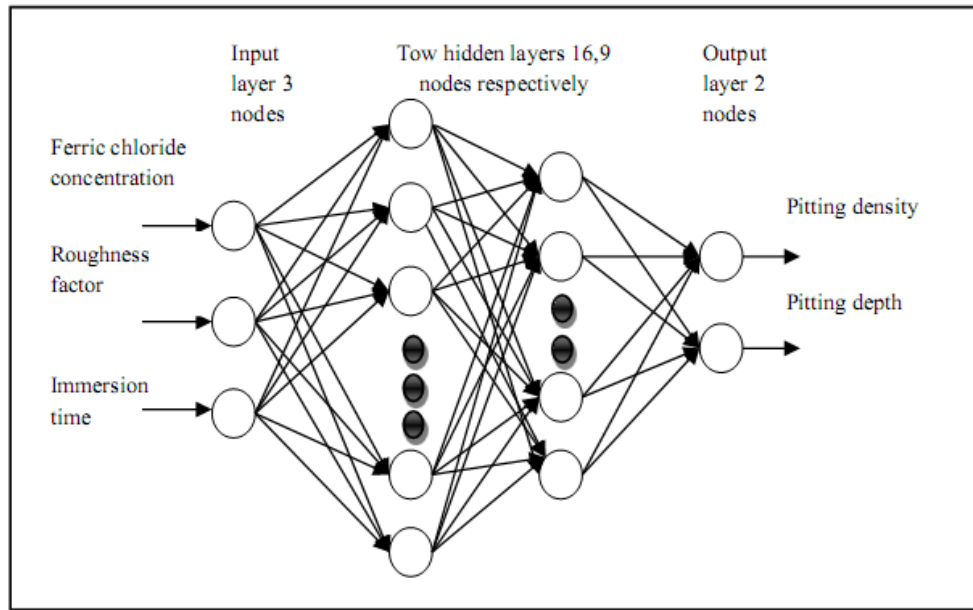


Figure1 . The architecture of ANN model.

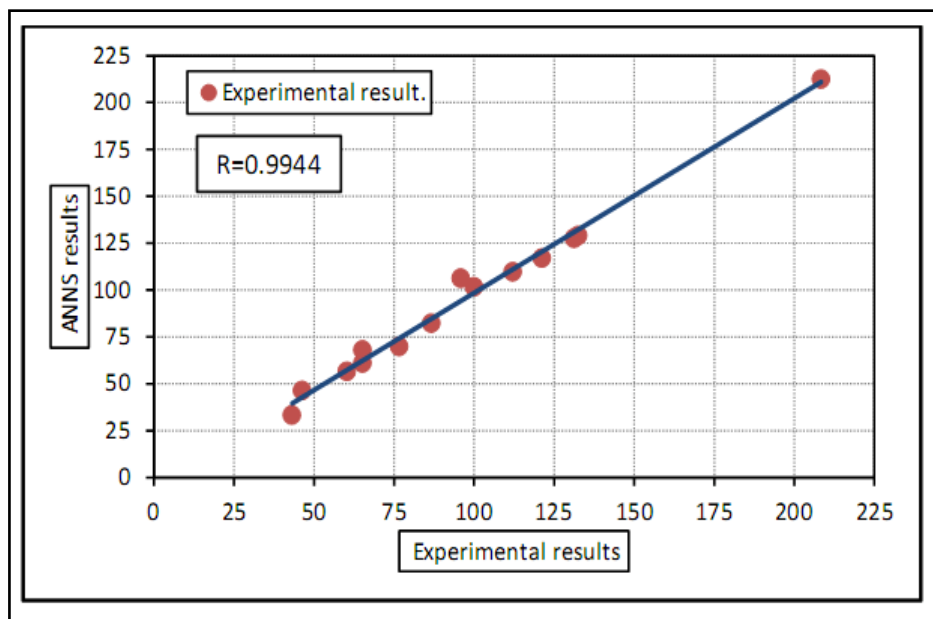


Figure 2. The results of the ANN model and the experimental results utilizing the resilient backpropagation algorithm are compared.

4. RESULTS AND DISCUSSION

The development of irreversible electrochemical processes (metal dissolution) and mass transport by diffusion at the metallic structure–environment contact cause localized corrosion. Although pit rate propagation into metal is difficult to predict, metallurgical structure and initial geometry of the substrate eliminate their location and distribution (Codaro *et al.*, 2002). In



general, the pitting corrosion process in the laboratory is caused by localized dissolution generated by aggressive anions (Cl^-) of ferric chloride solutions on carbon steel samples. Examining the metal surface after exposure to various corrosive concentrations for various periods produces visible pits; it is evident that these concentrations of aggressive anions promote the creation of distinct pits. **Figs. (3a, and b)** appeared two specimens of Ra values approximately $6\mu\text{m}$ after being immersed for (120 hours) with (1, and 6% wt.) chloride solution respectively.

Pits might be small and deep, or large and shallow, isolated or so near together that they resemble a rough surface comparable to a uniform attack (**Codaro et al., 2002**). In the present study, the examined metal surface by optical microscope revealed that the observed pits along the cross-section of all specimens treated with corrosive solution are of a large number of circular and elliptical, as shown in **Fig.4**.

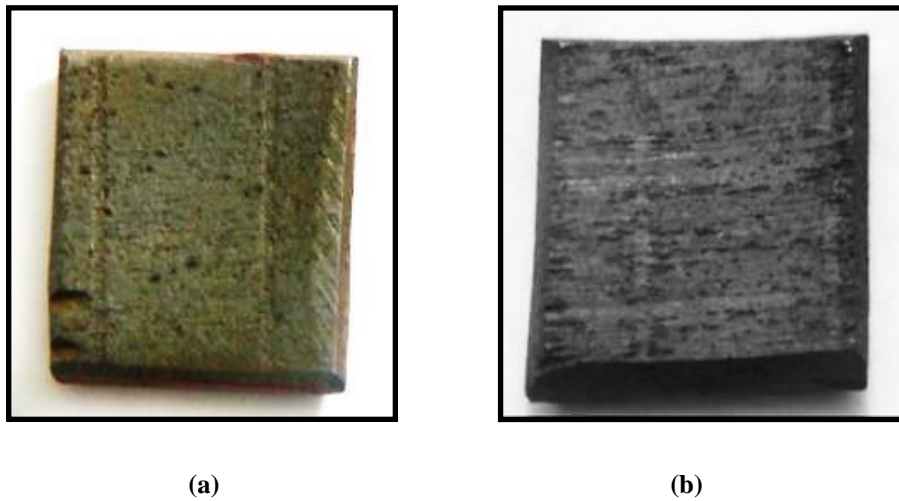


Figure 3. Pitting corrosion on CS specimen of approximate $6\mu\text{m}$ Ra value for 120 hr. immersion in a)(1% wt) ferric chloride solution. b) (6% wt.) ferric chloride solution.

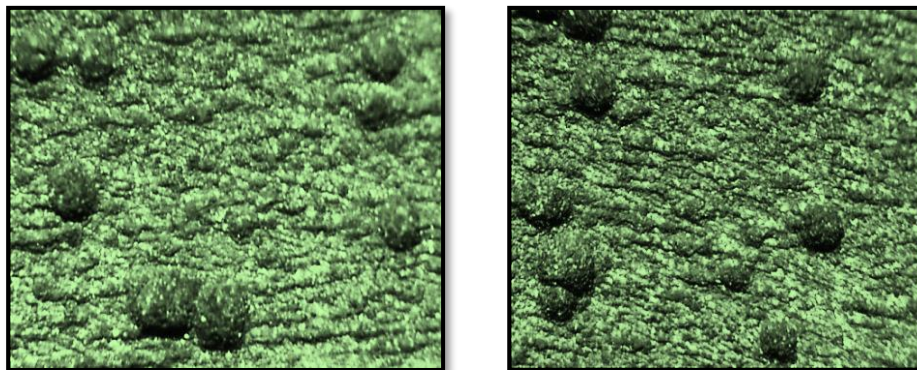


Figure 4. Micrograph showing the morphology of circular pitting corrosion for carbon steel (C-4130) (430X).



1. Effect of Roughness Factor: Pitting susceptibility is known to be influenced by the state of the metal surface. The larger the potential for pitting, the more homogenous the surface is, both chemically and physically. As a result, the number of pits is projected to decrease, while metal resistance to Pitting is expected to rise. Localized 'weak' places create surface roughness in the protective oxide film where a crucial Cl^- concentration exists or by homogeneities caused by surface preparation (Szklarska-Smialowska, 1986 and Bhandari et al., 2017). The effect of surface roughness factor on the pits at different ferric chloride concentrations on CS is shown in Figs. (5 and 6) respectively. Pits were shown to increase in direct proportion to both roughness factor and corrosive contents. The specimens of high Ra values (more than $7\mu\text{m}$) underwent severe attack by $[\text{Cl}^-]$ resulted in producing a large number of pits (i.e., high pitting density), and these pits are very close to each other. The merging of these pits together over the entire surface caused loss of metal thickness, and the metal surface seemed to be removed by general corrosion. Pitting nucleation is more likely on rougher specimen surfaces, resulting in a higher metastable pitting rate in this study (M. Mohammad, J. Hammadi, and M. Lafta, 2012 and Tang et al., 2019). By comparing the four different concentrations of corrosive solutions on CS, it's evident that increasing the concentration led to an increase in pit densities and depths values. At high corrosive concentrations (5 and 6 %wt.) and with a high Ra value and immersion duration of 96 hours, it is evident that in both two cases, a depression in the final stages was observed. This depression can be attributed to the restriction of the corrosive action of $[\text{Cl}^-]$ ions which are strongly restricted by the neighboring ions present in a large number of similar charges.

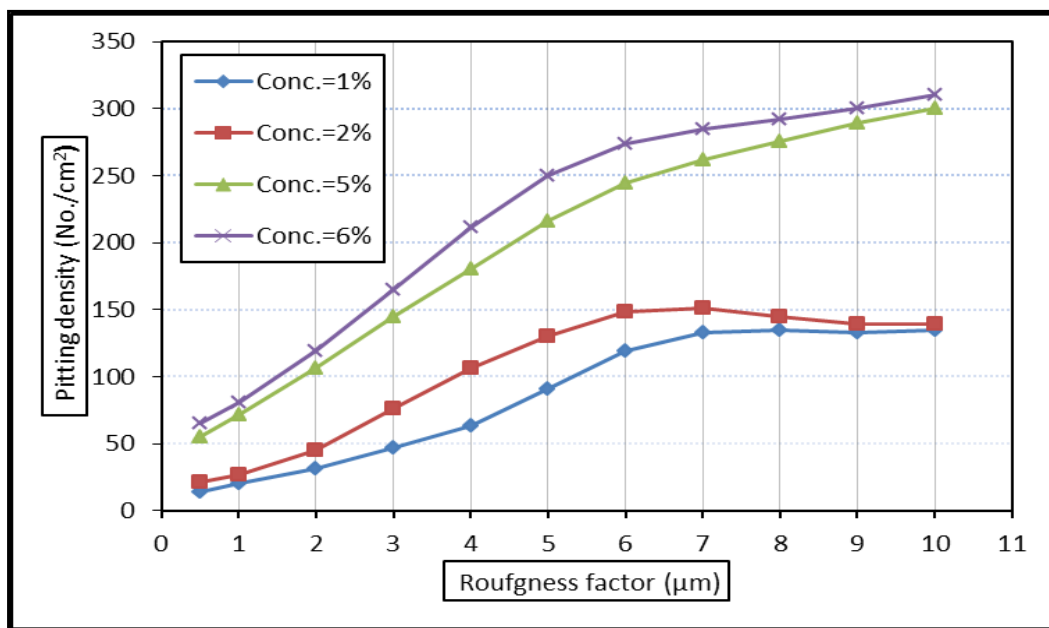


Figure 5. For (C-4130) carbon steel with different roughness factor, pitting density was calculated after a 96-hour immersion duration.

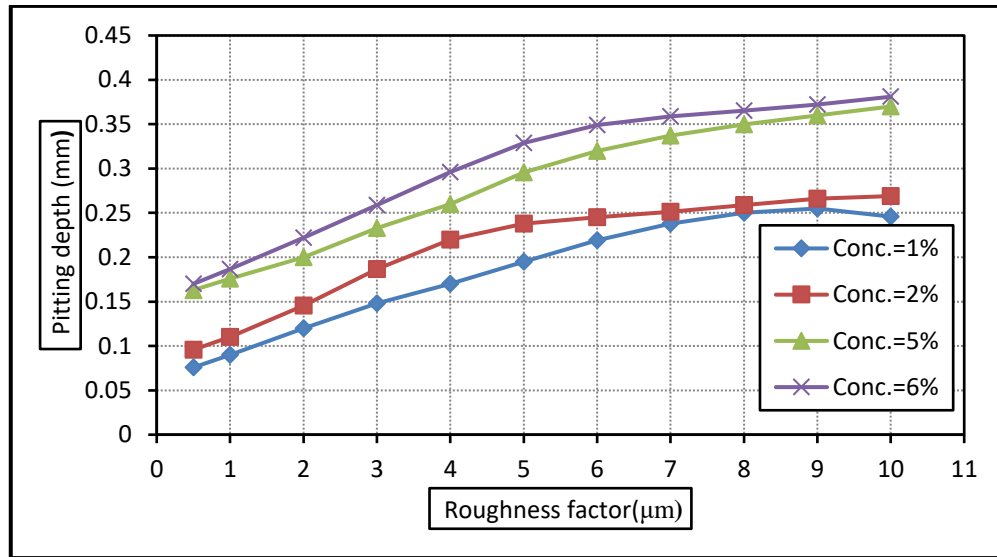
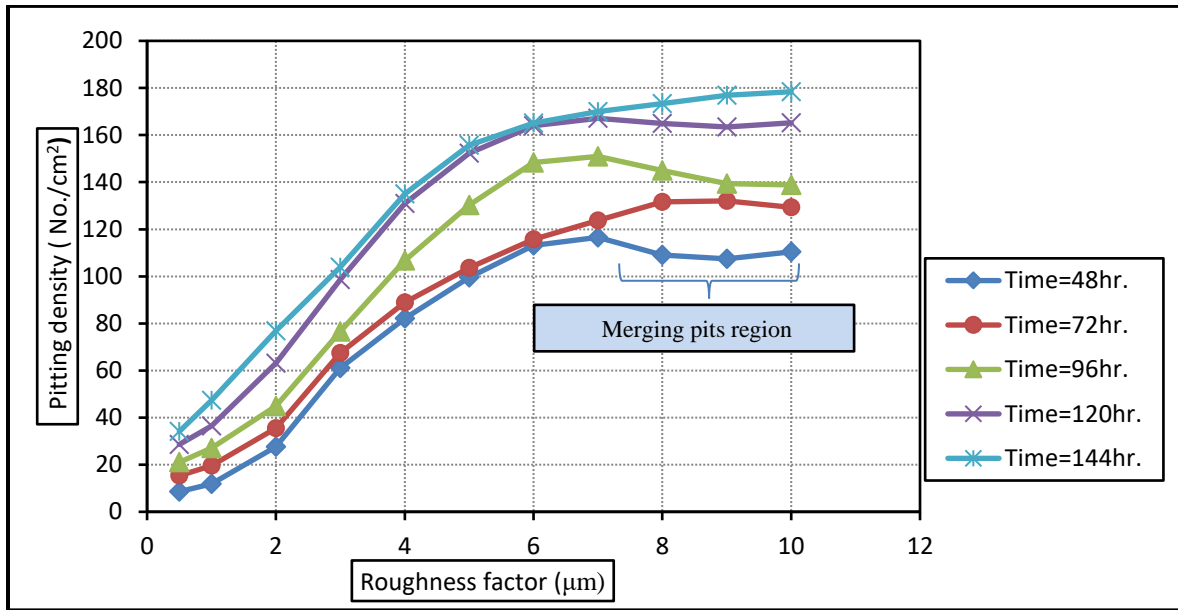
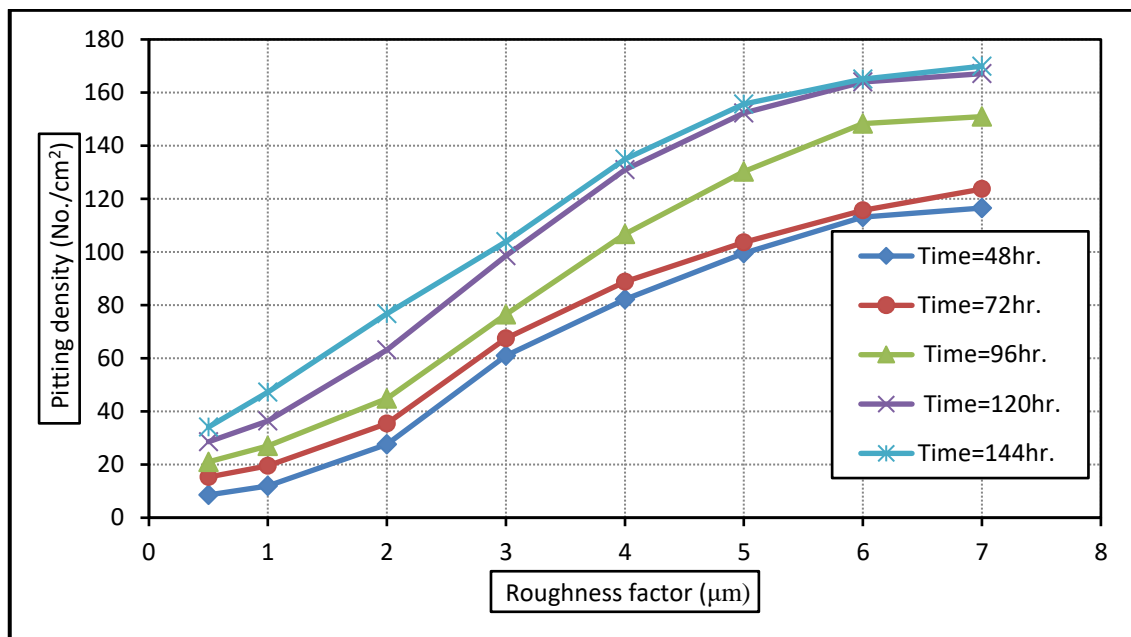


Figure 6. Pitting depth corresponding to roughness factor at 96 hour immersion time for (C-4130) carbon steel.

- 2. Effect of Immersion Time:** The ASTM G48 recommends a 72-hour test time, although other researchers (Bhandari et al., 2017 and M.Mohammad, J. Hammadi, and M. Lafta, 2012) had found to be particularly effective 24 hours, 48 hours, and 196 hours to 30 days. The effect of the roughness factor on the pitting at different immersion durations for (C-4130) CS is shown in Figs. (7 and 8). It is evident that there is an increase in pitting with increasing immersion durations and roughness factors. Although, specimens with high Ra values showed apparent deviations' in the measured Ra values after the corrosion process.

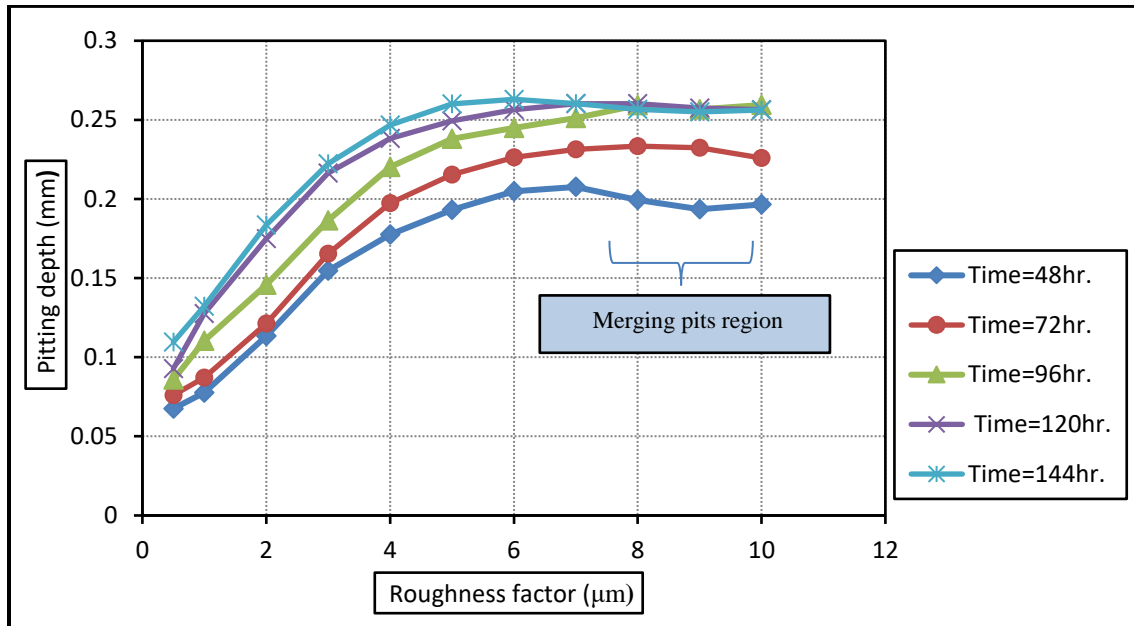


(a)

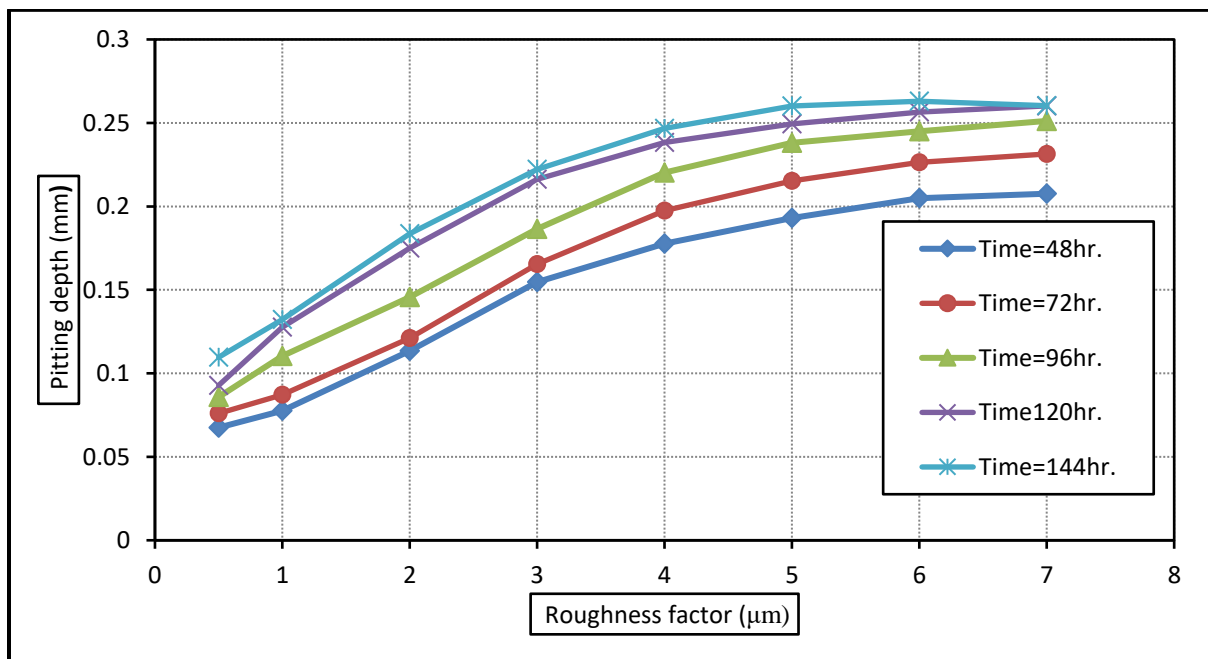


(b)

Figure 7. For (C-4130)carbon steel, pitting density corresponding to roughness factor at 2.0 percent ferric chloride concentration a) Ra value (1-10m). b) Ra value (1-7m) in the absence of pits merging.



(a)



(b)

Figure 8.: For (C-4130) carbon steel, pitting depth corresponding to roughness factor at 2.0 percent ferric chloride concentration. a) The Ra value (1-10m). b) Ra value (1-7m) in the absence of pits merging.

3. Effect of Ferric Chloride Concentration: Pits form and are always covered by corrosion products on a microscale. As a result, Pitting is one of the most destructive and unnoticeable kinds of metal corrosion. When steel is subjected to aqueous conditions containing chloride



ions, pitting corrosion is widespread. The chloride anion is the most frequent hostile ion found in many natural and industrial environments, including seawater. Pitting corrosion has long been regarded as one of the most severe operating issues in power plants and chemical plants (Bhandari et al., 2016, Khadom et al., 2015, and Krzemie et al., 2016). There are two sets of graphs that can be used to explain the effect of corrosive solution concentration on pitting corrosion characteristics; pitting with corrosive concentration at different immersion durations (48, 72, 96, 120, 144 h) with a roughness factor of 6 μm for (C-4130) CS, Figs. (9 and 10). Pitting depth and density increased, according to the study, directly with increasing corrosive concentrations, as corrosion rate increased with the increased activity of aggressive anions (Abd El Haleem et al., 2010) and Shakir et al., 2018).

To explain the mechanism of pitting corrosion, several consistent hypotheses have been proposed. Pit formation is thought to be caused by chlorides ions penetrating, inclusions, intermetallic particles, physical modifications of the surface (fine scratches, for example) generated by mechanical rolling, polishing, grinding treatments, or the passage of shaping tools. It causes locations in which Cl^- ions can easily penetrate metal.

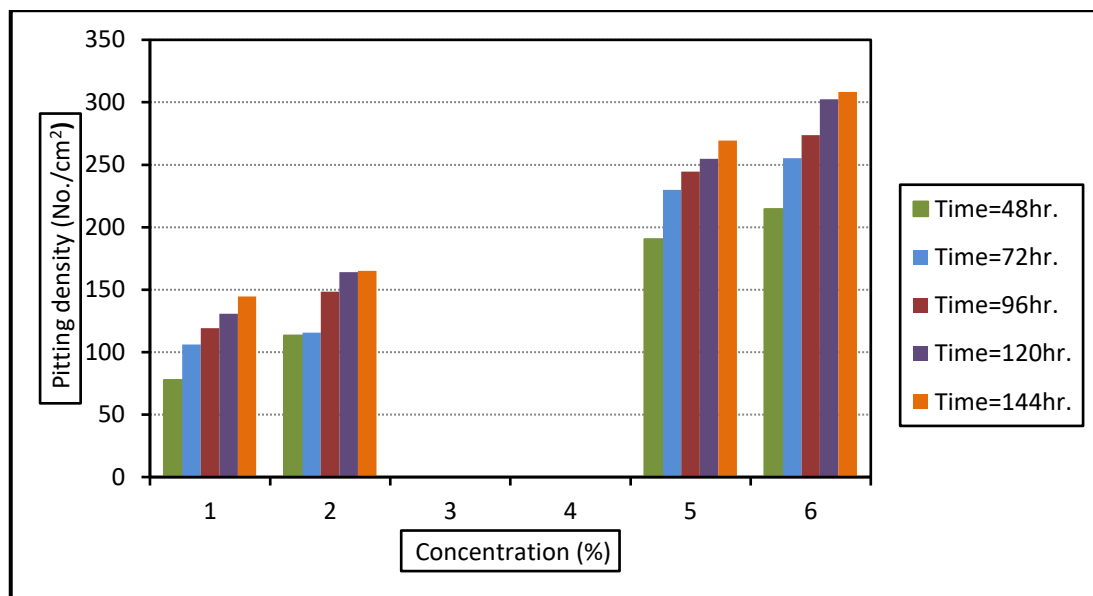


Figure 9. Pitting density with concentration at roughness factor of 6 μm for (C-4130) carbon steel.

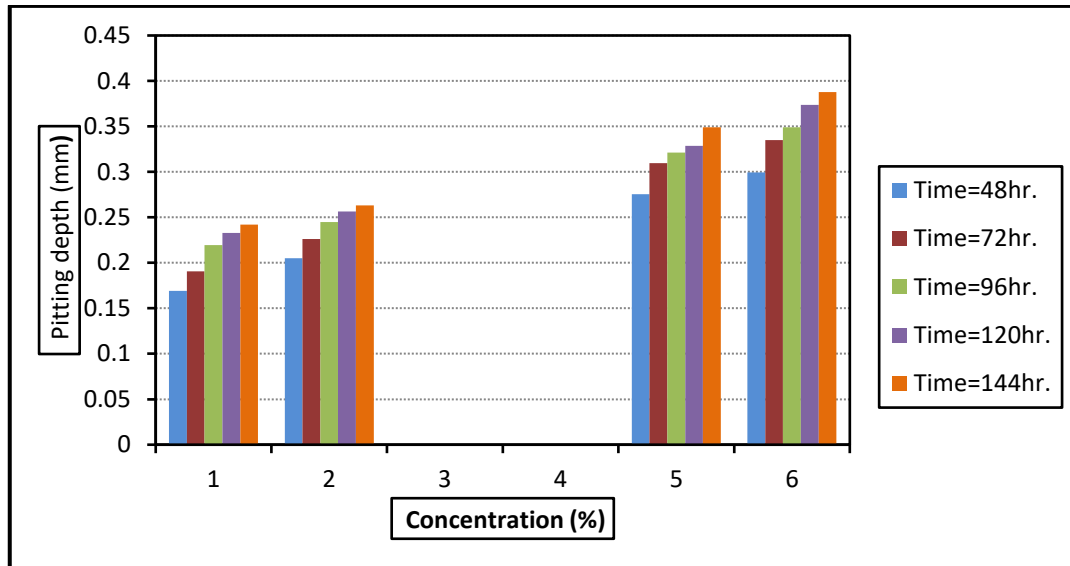


Figure 10. Pitting depth with concentration at roughness factor of $6\mu\text{m}$ for (C-4130) carbon steel.

5. CONCLUSIONS and RECOMMENDATION

The following are the most important conclusions that can be made from this research:

1. Growth in pitting density and depth was seen when corrosive content was increased with increased soaking time.
2. It was discovered that as the roughness factor increased, pitting density and pitting depth increased.
3. Artificial neural network models have been found to be highly successful in predicting pitting corrosion features. The outcomes were found to be in good agreement with those achieved from laboratory tests.

It was advised to use ANNS to predict pitting characterization when one of the protection methods, such as inhibitors, is to be used and determine the protection percentage. In addition, many critical factors affect localized corrosion in general and pitting corrosion in a specific manner that is not considered in this study, such as temperature and surface impurities, which should be taken into account.

ACKNOWLEDGMENT

The authors gratefully acknowledge the contributions of (Dr. Haider Maath Mohammed) for his support to complete this work.

REFERENCES

- Abd El Haleem, S. M. et al., 2010. Environmental factors affecting the corrosion behavior of reinforcing steel II. Role of some anions in the initiation and inhibition of pitting corrosion of steel in $\text{Ca}(\text{OH})_2$ solutions', *Corrosion Science*, 52(2), pp. 292–302.



DOI: 10.1016/j.corsci.2009.09.004.

- ASTM, G48, 2005 Standard Test Methods for Pitting and Crevice Corrosion Resistance of Stainless Steels and Related Alloys by the Use of Ferric Chloride Solution, Annual Book of ASTM Standards, ASTM International.
- ASTM, G46, 2005 Standard Guide for Examination and Evaluation of Pitting Corrosion 1, Annual Book of ASTM Standards.
- Bhandari, J., Khan, F., Abbassi, R., Garaniya, V., Ojeda, R., 2015. Modeling of Pitting Corrosion in Marine and Offshore Steel Structures-A Technical Review. Journal of Loss Prevention in the Process Industries, 37, 39–62. DOI:10.1016/j.jlp.2015.06.008.
- Bhandari J., Lau S., Abbassi R., Garaniya V., Ojeda R., Lisson D., and Khan. F., 2017. Accelerated Pitting Corrosion Test of 304 Stainless Steel using ASTM G48 Experimental Investigation and Concomitant Challenges, Loss Prevention in the Process Industries, DOI: 10.1016/j.jlp.2017.02.025.
- Boucherit, M. N. and Tebib, D., 2005. A study of carbon steels in basic pitting environments, Anti-Corrosion Methods and Materials, 52(6), pp. 365–370. DOI: 10.1108/00035590510624703.
- Boucherit, M. N. et al. 2019. Modeling input data interactions for the optimization of artificial neural networks used in the prediction of pitting corrosion, Anti-Corrosion Methods and Materials, 66(4), pp. 369–378. DOI: 10.1108/ACMM-07-2018-1976.
- Choi, Y.-S., Shim, J.-J., and Kim, J.-G., 2005 Effects of Cr, Cu, Ni and Ca on the Corrosion Behavior of Low Carbon Steel in Synthetic Tap Water. J. Alloy Comp. 391, 162–169. DOI:10.1016/j.jallcom.2004.07.081
- Codaro, E. N. et al., 2002. An image processing method for morphology characterization and pitting corrosion evaluation, Materials Science and Engineering A, 334(1–2), pp. 298–306. DOI: 10.1016/S0921-5093(01)01892-5.
- Ghidini, T., and Dalle Donne, C., 2009. Fatigue Life Predictions Using Fracture Mechanics Methods. Eng. Fracture Mech., 76 (1), 134–148. DOI:10.1016/j.engfracmech.2008.07.008.
- Jiménez-Come, M. J. et al., 2015. Characterization of pitting corrosion of stainless steel using artificial neural networks, Materials and Corrosion, 66(10), pp. 1084–1091. DOI: 10.1002/maco.201408173.
- Hornik, K., Stinchcombe, M., White, H., 1989. Multilayer feedforward networks are universal approximators. Neural Network 2, 359–366.
- Khadom, A.A., Hassan, A.F., Abod, B.M., 2015. Evaluation of environmentally



friendly inhibitor for galvanic corrosion of steel–copper couple in petroleum wastewater. *Process Safety and Environmental Protection* 98, 93-101.

- Kh. Hussein, 2015. Application of Box-Behnken Method Based ANN-GA to Prediction of wt % of Doping Elements for Incoloy 800H Coated Coated by Aluminizing-Chromizing, *Journal of Engineering*, 21(9).
- Kolawole, S. K., Kolawole, F. O., Enegele, O. P., Adewoye, O. O., Soboyejo, A. B. O., and Soboyejo, W. O., 2016. Pitting Corrosion of a Low Carbon Steel in Corrosive Environments: Experiments and Models. *Amr* 1132, 349–365. DOI:10.4028/www.scientific.net.
- Krzemień, A., Więckol-Ryk, A., Smoliński, A., Koteras, A., Więclaw-Solny, L., 2016 Assessing the risk of corrosion in amine-based CO₂ capture process. *Journal of Loss Prevention in the Process Industries* 43, 189-197.
- Li, W.-f., Zhou, Y.-j., and Xue, Y., 2012. Corrosion Behavior of 110S Tube Steel in Environments of High H₂S and CO₂ Content, *J. Iron Steel Res. Int.* 19, 59–6, DOI:10.1016/S1006-706X(13)60033-3.
- M.E.A. BenSeghier et al., 2021. Advanced intelligence frameworks for predicting maximum pitting corrosion depth in oil and gas pipelines, *Process Safety and Environmental Protection*, 147, 818-833
- M. Mohammad, H., J. Hammadi, N., and M. Lafta, R. 2012. Prediction of Pitting Corrosion Characteristics using Artificial Neural Networks, *International Journal of Computer*.
- Qu Z., Tang D., Wang Z., Li X., Chen H., and Lv Y., 2021. Pitting Judgment Model Based on Machine Learning and Feature Optimization Methods. *Frontiers in Materials*. Volume 8. Article 733813. DOI: 10.3389/fmats.2021.733813. www.frontiersin.org.
- Shakir, I. K. et al., 2018. Pitting Corrosion Behavior of 304 SS and 316 SS Alloys in Aqueous Chloride and Bromide Solutions, *Journal of Engineering*, 24(1), pp. 53–69.
- Szklarska-Smialowska, Z., 1986 Pitting corrosion of metals. National Association of Corrosion Engineers.
- Tang, Y. et al., 2019 Effect of surface roughness on pitting corrosion of 2205 duplex stainless steel investigated by electrochemical noise measurements, *Materials*, 12(5). DOI: 10.3390/ma12050738